A model of interactions between radiation-induced oxidative stress, protein and DNA damage in *Deinococcus radiodurans*

Igor Shuryak[a] and **David J. Brenner**[a,*]

[a]Center for Radiological Research, Columbia University Medical Center, New York, NY

Abstract

Ionizing radiation triggers oxidative stress, which can have a variety of subtle and profound biological effects. Here we focus on mathematical modeling of potential synergistic interactions between radiation damage to DNA and oxidative stress-induced damage to proteins involved in DNA repair/replication. When sensitive sites on these proteins are attacked by radiation-induced radicals, correct repair of dangerous DNA lesions such as double strand breaks (DSBs) can be compromised. In contrast, if oxidation of important proteins is prevented by strong antioxidant defenses, DNA repair may function more efficiently. These processes probably occur to some extent even at low doses of radiation/oxidative stress, but they are easiest to investigate at high doses, where both DNA and protein damage are extensive. As an example, we use data on survival of *Deinococcus radiodurans* after high doses (thousands of Gy) of acute and chronic irradiation. Our model of radiogenic oxidative stress is consistent with these data and can potentially be generalized to other organisms and lower radiation doses.

Keywords

mathematical model; DNA repair; protein oxidation; dose response; clonogenic survival; bacteria; Deinococcus radiodurans

1. Introduction

Ionizing radiation can damage all important cellular components, including DNA and proteins, both through direct ionization and through induction of oxidative stress. Radiogenic damage to DNA, such as double strand breaks (DSBs), which are typically difficult to repair and contribute greatly to clonogenic cell death, has been extensively studied (Barendsen, 1994; Iliakis et al., 2004; Kasten-Pisula et al., 2005; Saleh and El-Awady, 2005; Ward, 1990). Radiation-induced oxidative stress, which results in oxidation of proteins, lipids, and nucleotides, can have a variety of subtle and profound biological consequences, which are drawing increasing attention. For example, oxidative stress triggered by even quite low doses of radiation can produce an alteration of the cellular redox balance, which lasts for substantial time after exposure and may contribute to bystander effects, genomic instability, modified gene expression, elevated mutagenesis rates, changes in cell survival, proliferation, and differentiation (Azzam et al., 2002; Forman et al., 2002; Haddad, 2004; Hei, 2006; Mikkelsen,

2004; Rugo et al., 2002; Sangsuwan and Haghdoost, 2008; Schimmel and Bauer, 2002; Spitz et al., 2004; Tominaga et al., 2004).

Within this vast and complicated array of effects of radiogenic oxidative stress, in this article we focus on one aspect – potential interactions between oxidative damage to proteins and DNA damage repair. When sensitive sites on proteins involved in DNA repair and replication are oxidized by radiation-induced reactive oxygen and nitrogen species (ROS and RNS), the activity and fidelity of these proteins are altered, which may impede correct repair of DNA damage such as DSBs, enhancing cell death and mutagenesis (Adams et al., 1979; Bisby et al., 1982; Culard et al., 2003; Daly, 2009; Daly et al., 2007; Eon et al., 2001; Ghosal et al., 2005; Goodhead and Nikjoo, 1987; Kowalczyk et al., 2008; Saha et al., 1992). Such phenomena probably occur to some extent even at relatively low doses of radiation/oxidative stress (e.g. (Montaner et al., 2007)). However, they are easiest to investigate at high doses, where both DNA and protein damage are extensive (Adams et al., 1979; Bisby et al., 1982; Culard et al., 2003; Eon et al., 2001; Gerard et al., 2001; Goodhead and Nikjoo, 1987; Jolivet et al., 2006; Kowalczyk et al., 2008; Liu et al., 2003; Zahradka et al., 2006; Zimmermann et al., 1994), and interactions between them are probably most pronounced.

A good opportunity to study this aspect of radiation-induced oxidative stress is provided by certain prokaryotes, which have been evolutionarily optimized for coping with genotoxic agents such as desiccation, oxidative stress and UV radiation, and are, therefore, highly resistant to ionizing radiation (Blasius et al., 2008; Shukla et al., 2007). The best studied organism in this category is the bacterium *Deinococcus radiodurans*, which can survive acute exposure to several kGy of γ– or high-LET radiation without loss of viability and can proliferate at a normal rate under chronic γ-radiation at 50 or 60 Gy/h (Brim et al., 2006; Daly et al., 2004; Dewey, 1969; Lange et al., 1998; Zimmermann et al., 1994).

Here we propose a simple mathematical model, which is intended to investigate the potential synergistic relationship between oxidative stress, protein and DNA damage, using data on *D. radiodurans* as an example. The model is consistent with the observed patterns of cell survival for this organism under chronic irradiation and after acute exposures (e.g., (Battista et al., 1999; Blasius et al., 2008; Brim et al., 2006; Daly, 2006; Daly, 2009; Daly et al., 2007; Daly et al., 2004; Dewey, 1969; Ghosal et al., 2005; Hess, 2003; Jolivet et al., 2006; Lange et al., 1998; Liu et al., 2003; Makarova et al., 2001; Makarova et al., 2007; Mennecier et al., 2006; Shukla et al., 2007; White et al., 1999; Zahradka et al., 2006; Zhang et al., 2005; Zimmermann et al., 1994), reviewed by (Blasius et al., 2008; Daly, 2009)) and can assist in the interpretation of these patterns. Potentially, models such as the one presented here can enhance the understanding of radiation-induced oxidative stress at lower radiation doses and in other organisms, because the main model concepts are probably generalizable.

2. Model assumptions and implementation

The main model assumptions are shown schematically in Fig. 1. More detailed discussion of these assumptions and their mathematical implementation is provided below.

2.1. Protein oxidation

During irradiation, reactive oxygen species and other radicals and oxidants (generically called *ROS* here) are generated, and can damage proteins (called *PR* here) which are needed for correct repair of DNA damage. Scavenging of radicals is accomplished by enzymatic and non-enzymatic antioxidants (generically called *A* here). Some radicals are also assumed to be inactivated by reacting with molecules in the cell which are not critical for survival; this mechanism is approximated by a first-order process. To reduce the number of adjustable parameters, we neglect several potentially substantial phenomena such as non-reversible ROS

scavengers, a second-order process whereby ROS are inactivated by reacting with each other, ROS production under background conditions, multiple types of antioxidants and DNA repair proteins, etc. This set of assumptions is represented by the following system of differential equations:

$$\mathrm{dROS}(t)/\mathrm{dt} = c_1\,R - c_2\,\mathrm{ROS}(t)\,A(t) - c_3\,\mathrm{ROS}(t)$$
$$\mathrm{dA}(t)/\mathrm{dt} = -c_2\,\mathrm{ROS}(t)\,A(t) + c_4\,\mathrm{ROS}C(t)$$
$$\mathrm{dROS}C(t)/\mathrm{dt} = c_2\,\mathrm{ROS}(t)\,A(t) - c_4\,\mathrm{ROS}C(t)$$
$$\mathrm{dPR}(t)/\mathrm{dt} = c_5 - [c_6 + c_7\,\mathrm{ROS}(t)]\,\mathrm{PR}(t) \tag{1}$$

Here A is the active form of the antioxidant, $ROSC$ is the ROS-antioxidant complex (the temporarily inactive form of the antioxidant, which can be regenerated back to the active form A), and R is the radiation dose rate. The parameter interpretations, also presented in Table 1, are: $c_1 = ROS$ production by radiation; $c_2 = ROS$ removal by antioxidant; $c_3 = ROS$ removal by first-order kinetics; $c_4 =$ regeneration of active antioxidant from the ROS-antioxidant complex; $c_5 =$ protein production; $c_6 =$ protein degradation (the equilibrium protein concentration under background conditions $= c_5/c_6$); $c_7 =$ protein inactivation by ROS.

The system in Eq. (1) can be simplified by applying an equilibrium assumption, i.e. that the active and inactive forms of the antioxidant (A and $ROSC$, respectively) always exist in equilibrium and the sum of their concentrations is equal to A_{tot}, where A_{tot} is the total antioxidant concentration, which is assumed to be constant (because radiation exposure is assumed to be severe enough for maximal induction of antioxidant defenses). Solving for the equilibrium concentrations of A and $ROSC$ and substituting the solutions into Eq. (1) generates the following system of equations:

$$\mathrm{dROS}(t)/\mathrm{dt} = c_1\,R - c_2\,c_4\,A_{\mathrm{tot}}\,\mathrm{ROS}(t)/[c_4 + c_2\,\mathrm{ROS}(t)] - c_3\,\mathrm{ROS}(t)$$
$$\mathrm{dPR}(t)/\mathrm{dt} = c_5 - [c_6 + c_7\,\mathrm{ROS}(t)]\,\mathrm{PR}(t) \tag{2}$$

Assuming that the kinetics of ROS production and removal are faster than those of protein turnover, Eq. (2) can also be simplified by assuming that ROS always exist at an equilibrium concentration ROS_{eq}, which is given by the following expression:

$$\mathrm{ROS}_{\mathrm{eq}} = (c_2\,X_1 - c_3\,c_4 + X_3^{\frac{1}{2}})/(2\,c_2\,c_3),$$
$$\text{where } X_1 = c_1\,R - c_4\,A_{\mathrm{tot}}, \qquad X_2 = c_1\,R + c_4\,A_{\mathrm{tot}},$$
$$X_3 = c_2^2\,X_1^2 + 2\,c_2\,c_3\,c_4\,X_2 + (c_3\,c_4)^2 \tag{3}$$

It is expected that at low radiation dose rates the antioxidant concentration is sufficient to counteract ROS production, thereby maintaining ROS_{eq} at low values. At higher dose rates, the antioxidant becomes saturated and can no longer counteract accumulation of ROS, so ROS_{eq} is determined mainly by the (slower) first-order removal process and can rise to very high values. This behavior is shown in Fig. 2 using parameter values from Table 1.

The protein inactivation kinetics by ROS can then be estimated by substituting Eq. (3) into Eq. (2), using ROS_{eq} in place of $ROS(t)$. The equilibrium concentration of active protein, PR_{eq}, can then be derived:

$$PR_{eq}=2\,c_2\,c_3\,c_5/(c_2\,[\,c_7\,X_1+2\,c_3\,c_6]-c_7\,[\,c_3\,c_4-X_3^{\frac{1}{2}}]),$$
$$\text{where } X_1=c_1\,R-c_4\,A_{tot}, \qquad X_2=c_1\,R+c_4\,A_{tot},$$
$$X_3=c_2^{\,2}\,X_1^{\,2}+2\,c_2\,c_3\,c_4\,X_2+(c_3\,c_4)^2 \tag{4}$$

As intuitively expected, PR_{eq} as function of radiation dose rate (Eq. (4)) behaves in an inverse manner to ROS_{eq} – at low dose rates the protein remains largely functional, protected by antioxidant mechanisms, and at higher dose rates it becomes progressively inactivated by ROS (Fig. 3). PR_{eq} does not show a very dramatic percentage decrease around the dose rate of 0.1 kGy/h, corresponding to the dramatic percentage increase in ROS_{eq} (compare Figs. 2 and 3), because the selected value of parameter c_7, which determines protein degradation by ROS, is small (i.e. it takes a lot of ROS to inactivate a substantial percentage of protein).

2.2. DNA damage

Radiation also generates multiple types of DNA damage, among which the most critical for cell survival are double strand breaks (DSB). In bacteria, antioxidants which protect proteins do not appear to protect DNA very well because different types of ROS may preferentially attack proteins vs. DNA (Daly et al., 2007). Consequently, the yield of DSBs per unit dose per base pair of DNA is similar in most bacteria under similar conditions (Gerard et al., 2001). Correct repair of DSBs (i.e. repair that is sufficient for cell survival, not necessarily for lack of mutation), however, is assumed to be dependent on the concentration of functional repair proteins (here generalized as PR). Of course, this set of assumptions, which is dictated by the need for reducing the number of model parameters, is highly simplistic and ignores multiple potentially important phenomena such as direct induction of DSBs by ROS, the existence of multiple types of DNA damage and damage repair proteins, etc. However, we believe that our assumptions capture some crucial aspects of the interactions between oxidative stress and DNA damage. They are modeled by the following differential equation, where c_8 is the constant for DSB production by radiation and c_9 is the correct repair constant:

$$dDSB(t)/dt=c_8\,R-c_9\,PR(t)\,DSB(t) \tag{5}$$

At a constant dose rate, the equilibrium number of DSBs per cell (DSB_{eq}) can be calculated by substituting PR_{eq} in place $PR(t)$ of into Eq. (5). The result is Eq. (6) below:

$$DSB_{eq}=c_8\,R\,[\,c_2\,(2\,c_3\,c_6+c_7\,X_1)-c_3\,c_4\,c_7+c_7\,X_3^{\frac{1}{2}}]/(2\,c_2\,c_3\,c_5\,c_9),$$
$$\text{where } X_1=c_1\,R-c_4\,A_{tot}, \qquad X_2=c_1\,R+c_4\,A_{tot},$$
$$X_3=c_2^{\,2}\,X_1^{\,2}+2\,c_2\,c_3\,c_4\,X_2+(c_3\,c_4)^2 \tag{6}$$

The behavior of DSB_{eq} as function of dose rate is shown in Fig. 4, and is consistent with the behavior of PR_{eq} described earlier. Given the default parameter values (Table 1), Eq. (6) is well approximated by the linear-quadratic expression $DSB_{eq} = 5\,R + 58/15\,R^2$, where R is in kGy/h.

2.3. Effects of an acute radiation exposure

By the time radiation exposure is over, i.e. when $t = Dose/R$, where $Dose$ is the total radiation dose, the concentration of active protein (PR_d) can be calculated by using Eqs. (2) and (3) and assuming that the protein concentration before exposure was in equilibrium (i.e. $PR(t{=}0) = c_5/c_6$):

$$PR_d = c_5 \left[2\, c_2\, c_3\, c_6/Y_2 + c_7\, (Y_1^{\frac{1}{2}} + c_2\, X_1 - c_3\, c_4)\right] Y_2/[\, c_6\, (c_7\, Y_1^{\frac{1}{2}}$$
$$+ c_7\, (c_2\, X_1 - c_3\, c_4) + 2\, c_2\, c_3\, c_6)], \text{ where } X_1 = c_1\, R - c_4\, A_{\text{tot}},$$
$$Y_1 = c_4^{\ 2}\, (c_2\, A_{\text{tot}} + c_3)^2 + 2\, c_1\, c_2\, c_4\, R\, (c_3 - c_2\, A_{\text{tot}}) + (c_1\, c_2\, R)^2,$$
$$Y_2 = \exp[\, -\text{Dose}\, (c_7\, Y_1^{\frac{1}{2}} + c_2\, (2\, c_3\, c_6 + c_7\, X_1) - c_3\, c_4\, c_7)/(2\, c_2\, c_3\, R)] \tag{7}$$

The behavior of PR_d as function of dose and dose rate is shown in Fig. 5. At very low dose rates, where damage to protein by ROS is limited by antioxidant defenses, most of the protein remains active regardless of the cumulative radiation dose. At very high dose rates, the protein becomes inactivated as function of dose in an approximately first-order manner.

Assuming the irradiation is acute for the purposes of DNA repair (i.e. the total dose is delivered in such a short time that no DSBs can be repaired during exposure), the number of DSBs just after exposure is: $DSB_d = c_8\, Dose$. The protein concentration just after exposure is PR_d, given by Eq. (7). Over time after exposure (t), DSB repair and protein turnover are described by the following differential equations:

$$dDSB(t)/dt = -\, c_9\, PR(t)\, DSB(t)$$
$$dPR(t)/dt = c_5 - c_6\, PR(t) \tag{8}$$

Eq. (8) can be solved analytically to yield the following expressions (Eq. (9) below), where PR_d is given by Eq. (7):

$$DSB(t) = c_8\, \text{Dose} \exp[\, -c_9\, (c_6\, (c_5\, t + PR_d) + (c_5 - c_6\, PR_d) \exp[\, -c_6\, t] - c_5)/c_6^{\ 2}]$$
$$PR(t) = [\, (c_6\, PR_d - c_5) \exp[\, -c_6\, t] + c_5]/c_6 \tag{9}$$

The cell survival predicted for some finite time available for repair (T_{rep}) is defined, according to standard assumptions that a single incorrectly repaired DSB is lethal to the cell, as $S = \exp[-DSB(T_{rep})]$, where $DSB(t)$ is given by Eq. (9). During exponential growth, *D. radiodurans* typically grows as a mixture of tetracocci (4-cell clusters) and diplococci (2-cell clusters) in an approximately 75:25% distribution (Daly et al., 2004). So, the survival for colony-forming units (cell clusers), which is assessed experimentally, is the following function of cell survival: $S_{cfu} = 0.75\, (1 - (1 - S)^4) + 0.25\, (1 - (1 - S)^2)$. The behavior of S_{cfu} as function of radiation dose, compared with observed data points for *D. radiodurans* exposed to γ-radiation in complete growth medium (Daly et al., 2004), is shown in Fig. 6.

2.4. Parameter values and model sensitivity analysis

The model contains 11 parameters ($c_1 - c_9$, A_{tot} and T_{rep}), only three of which (the DSB production rate by radiation $c_8 = 10.0$ breaks×cell^{-1}×kGy^{-1}, the DSB repair constant $c_9 = 1.5$ concentration^{-1}×h^{-1}, and the time available for repair $T_{rep} = 4.0$ h) could be easily estimated from the literature (Battista et al., 1999; Blasius et al., 2008; Daly, 2006; Daly, 2009; Daly et al., 2007; Daly et al., 2004; Ghosal et al., 2005; Jolivet et al., 2006; Zahradka et al., 2006). The constants for ROS production by radiation (c_1), ROS removal by antioxidant (c_2) and regeneration of active antioxidant (c_4) were set to large values (Table 1) because there processes are very rapid compared with protein turnover and DSB repair kinetics. Their actual values are not particularly important, given a constant ratio between them. The remaining parameters were freely adjusted to fit the data.

More insight into model behavior can be gained by measuring the sensitivity of model predictions to changes in each parameter. We performed both local and global sensitivity

analyses. Local sensitivity was assessed by varying a given parameter by a selected factor (e.g. 1.5) above and below the default value, keeping all other parameters constant at their default values. Global sensitivity was estimated by calculating partial rank correlation coefficient (PRCC) for each parameter (described in the Appendix), according to the method reviewed by (Marino et al., 2008).

3. Results

The mathematical model presented here can qualitatively and quantitatively describe two processes thought to be important for survival of bacteria at high doses of ionizing radiation: DNA double strand break (DSB) repair and protein oxidation. The interactions of these processes under conditions of severe radiation-induced oxidative stress are analyzed. Model predictions using some parameter values estimated from the literature and using freely-adjusted values for the remaining parameters (Table 1) were consistent with the observed survival curve of *D. radiodurans* exposed to acute γ-radiation (Daly et al., 2004) (Fig. 6), and with the ability of *D. radiodurans* to grow under constant dose rates of 0.05 or 0.06 kGy/h (Brim et al., 2006;Daly et al., 2004;Lange et al., 1998) by preventing excessive accumulation of DNA and protein damage (Figs. 3, 4). As more information becomes available to estimate model parameters, the formalism can be tested more rigorously.

Local model sensitivity to varying the value of each parameter one at a time, keeping all other parameters at default values, was performed for colony-forming unit survival (S_{cfu}) after acute irradiation (Fig. 7), for equilibrium number of DSBs per cell (DSB_{eq}) under chronic irradiation (Fig. 8) and for normalized equilibrium concentration of active protein (PR_{eqF}) under chronic irradiation (Fig. 9). The parameters were varied by a factor of 5 in Figs. 8 and 9, so that changes in the predictions would be easily noticeable visually. In Fig. 7 a smaller factor of 1.5 was sufficient because the survival curve (S_{cfu}), which has an approximately exponential dependence on the number of DSBs, is logically more sensitive to changes in parameter values than is the number of DSBs.

For S_{cfu}, local sensitivity was also assessed numerically (Table 2) by estimating the effects of varying each parameter on the radiation dose required to reduce S_{cfu} to 90% (Dose$_{90}$), and on the Log$_{10}$ decrease in S_{cfu} at a dose of 20 kGy (Slope$_{20}$). Dose$_{90}$ is a measure of the length of the "shoulder" of the survival curve, and Slope$_{20}$ is a measure of the "terminal slope" of the survival curve. Additionally, global model sensitivity to each parameter was also estimated for DSB_{eq} and S_{cfu}, with more details provided in the Appendix (and Table A1).

As expected, sensitivity to a given parameter can be modulated by what outcome variable is tested (e.g. DSB_{eq} vs. S_{cfu}) and by radiation dose and dose rate. Globally, both DSB_{eq} and S_{cfu} were most sensitive to: DSB production and repair constants (c_8 and c_9, respectively), DSB repair protein production and degradation constants (c_5 and c_6, respectively), and the time available for DSB repair (T_{rep}). Sensitivity of DSB_{eq} to ROS production by radiation (c_1) and protein inactivation by ROS (c_7) was, as expected, relatively low at low dose rates, but increased at higher dose rates (Table A1). Local sensitivity studies support this (Figs. 8, 9). Such behavior can be attributed to the fact that, given our model parameters, at low dose rates ROS concentrations are relatively low, in part due to antioxidant protection, and DSBs at these dose rates are mostly generated directly by radiation. At high dose rates, however, ROS concentrations become high, and ROS-induced DSBs make an important contribution to DSB_{eq}.

The local sensitivity analysis (Table 2 and Figs. 7-9) also largely confirmed the intuitive role of each parameter in the model. For example, it showed that the constants for ROS production by radiation (c_1), ROS removal by first-order kinetics (c_3), protein inactivation by ROS (c_7),

and DSB induction by radiation (c_8) predominantly affect the slope of the survival curve at high doses. In contrast, the parameters for protein production and degradation (c_5 and c_6, respectively), the DSB repair constant (c_9), and the time available for DSB repair (T_{rep}) strongly affect both the high-dose slope, and the low-dose shoulder of the survival curve.

4. Discussion

Almost by definition, mathematical models are greatly simplified representations of complex biological processes. The model presented here focuses on the interactions between protein and DNA damage in the context of radiogenic oxidative stress, which have been suggested to be important for clonogenic survival of irradiated *D. radiodurans* and some other prokaryotes. Many aspects of this phenomenon, as well as multiple other factors known to be relevant for cell survival, have not been included in the model to improve its tractability and decrease the number of adjustable parameters. For example, for these reasons we neglected the following: metabolism-induced ROS, which can be important during and after irradiation (Daly et al., 2007; Ghosal et al., 2005); acceleration of protein turnover (e.g. degradation and excretion of damaged proteins and synthesis of their replacements) during and after irradiation (Blasius et al., 2008; Liu et al., 2003); and causes of cell death other than unrepaired/misrepaired DNA DSBs, e.g. severe global protein damage and activation of latent bacteriophages during DNA repair (Mennecier et al., 2006; Qiu et al., 2006). Also, it is important to note that parameter combinations other than the one we chose as the default (Table 1) may certainly be able to fit our selected data set just as well, particularly if the ratios between certain parameter values (e.g. between the ROS-related constants c_1-c_4) are kept constant. Additional data from future experimental studies will be needed to unambiguously determine these parameter values.

Despite its limitations, we believe that the model captures some crucial aspects of radiation-induced oxidative stress and its potentially synergistic relationship with DNA damage. In addition to being consistent with the selected experimental data set (clonogenic survival of *D. radiodurans* at different doses and dose rates), the model suggests some potentially useful insight and generalizations:

1. For chronic irradiation, the model predicts that oxidative stress (ROS accumulation) and its consequences such as DNA repair protein oxidation can be largely suppressed by protective antioxidants at sufficiently low dose rates, but exhibit a dramatic release from suppression beyond a certain "threshold" dose rate, where the antioxidant capacity is saturated and overwhelmed. Above this threshold, protein damage will accumulate rapidly, thereby compromising DNA repair and making cell survival and proliferation impossible. Using the semi-arbitrary parameters chosen here (Table 1), the threshold dose rate should lie in the range of 100 - 1000 Gy/h (Figs. 2-4). This prediction needs to be tested by additional experimental data. Currently, the growth of *D. radiodurans* under chronic exposure was assessed only for dose rates of 50 or 60 Gy/h (Brim et al., 2006; Daly et al., 2004; Lange et al., 1998), showing that under such conditions proliferation of this organism in complete growth medium is essentially unaffected. Assessing the proliferation capacity (or lack of it) of *D. radiodurans* under higher chronic dose rates can test whether or not a threshold dose rate exists and/or determine its value.

2. Because some parameters affect model predictions to different extents depending on dose rate, i.e. some are much more important at high dose rates and relatively unimportant at low dose rates or vice versa (Fig. 8), the ability of a given organism to counteract radiation effects at low dose rates and at high dose rates may not necessarily be correlated. In other words, if an organism is highly resistant to acute exposures, it may be quite sensitive to chronic irradiation, or the other way around. This is supported by mutants of *D. radiodurans* which exhibit wild-type survival after

acute exposures to several kGy, but cannot grow under chronic irradiation of 50-60 Gy/h, and vice versa (Hess, 2003). Also, other bacteria, such as *Enterococcus facium*, can grow well under 50 Gy/h, but are much more sensitive to acute exposures than *D. radiodurans* (Daly et al., 2004).

3. Similarly, the length of the shoulder and the steepness of the high-dose slope of the survival curve after acute irradiation may not necessarily be correlated, because they are determined to different extents by certain parameters (Table 2, Fig. 7). For example, it is possible for the model to generate a curve with a small shoulder and a shallow slope, or a large shoulder and a steep slope. This is qualitatively consistent with survival curve shape variability in *D. radiodurans* as function of radiation LET (Dewey, 1969) and composition of the growth medium (Daly et al., 2007;Daly et al., 2004;Zhang et al., 2005), because these factors can modulate ROS production by radiation, the number and complexity of DSBs induced per unit dose, cellular antioxidant concentrations (e.g. of manganese ions), the ability to repair DSBs, protein turnover rates, and other relevant parameters.

Of course, the current formalism is only a preliminary attempt to model the interactions between oxidative stress and DNA damage repair. However, we believe that the basic approach presented here may potentially be applied to other organisms and lower radiation doses, because the main concepts and assumptions (Fig. 1) were intended to be quite general. For example, it has been shown experimentally that in mammalian cells ROS are removed by a combination of saturable and first-order kinetics (Makino et al., 2008;Sasaki et al., 1998), as assumed in the current model. Potential interference of ROS with DNA repair by oxidation of sensitive sites on DNA repair proteins may not occur to the same extent at lower radiation doses as at high doses, but may be important in some systems even on a subtle level – e.g. if the endpoint of interest is cell mutagenesis (and potential consequent carcinogenesis), rather than cell survival, then even small defects in DSB repair may become substantial.

Certainly, details of the model equations may need to be modified for particular organisms and situations. It seems likely that to apply this approach to mammalian cells, the main assumptions outlined here can still be used, but additional aspects may need to be considered. For example, it may be necessary to model some of the eukaryote-specific complexities of ROS production and removal (e.g. the role of radiation-damaged mitochondria in generating ROS even after irradiation has ended, the role of non-reversible antioxidants such as histones, etc.) and DSB repair (e.g. several competing non-homologous end joining and homologous recombination pathways). Also, DNA damage types other than DSBs may need to be considered for studying cell mutagenesis and carcinogenesis.

Acknowledgments

Appendix

Because the number of adjustable model parameters is large, estimates of global parameter sensitivity using the partial rank correlation coefficient (PRCC) were performed for the equilibrium number of DSBs/cell (DSB_{eq}) as function of radiation dose rate (R), and for colony-forming unit survival (S_{cfu}) as function of radiation dose (D). The methodology of calculating and interpreting PRCCs is reviewed in detail by (Marino et al., 2008). Briefly, our procedure was as follows: For each dose or dose rate tested, 10,000 model simulations were performed. During each simulation, parameter values were determined by a log-normal distribution with the standard deviation equal to one order of magnitude (i.e. a 10-fold decrease or increase

compared with the default value of the given parameter). The simulated parameter values and the corresponding model predictions were rank-transformed in ascending order (i.e. assigned ranks of 1 to 10,000, with the smallest numbers having the lowest ranks). Then the partial correlation coefficient with the model predictions was calculated for each parameter by adjusting for the linear effects of the other parameters by linear regression.

This method measures global model sensitivity to each parameter. A large positive PRCC (i.e. approaching +1) indicates that increasing the value of the given parameter substantially increases the model prediction. The converse is true for a large negative PRCC (i.e. approaching -1). The results are shown in Table A1. Some of the main patterns suggested by these PRCC values are discussed in the main text. This information can supplement the local parameter sensitivity calculations described in the main text, in Table 2 and in Figs. 7-9.

Table A1

Estimates of global parameter sensitivity using partial rank correlation coefficient (PRCC), as described in the text, for the equilibrium number of DSBs/cell (DSB_{eq}) as function of radiation dose rate (R, kGy/h), and for colony-forming unit survival (S_{cfu}) as function of radiation dose (D, kGy). Each PRCC value is based on 10,000 simulations; the critical value for 5% significance (compared with zero) is ±0.0165.

Parameter	DSB_{eq}				S_{cfu}	
	R = 0.01	R = 0.05	R = 0.1	R = 5.0	D = 20	D = 25
c_1	0.130	0.249	0.305	0.576	-0.197	-0.199
c_2	-0.019	-0.017	-0.017	-0.006	0.010	0.007
c_3	-0.080	-0.166	-0.208	-0.494	0.202	0.201
c_4	-0.071	-0.106	-0.120	-0.147	0.034	0.035
c_5	-0.849	-0.817	-0.802	-0.745	0.639	0.635
c_6	0.834	0.781	0.748	0.478	-0.495	-0.483
c_7	0.087	0.166	0.211	0.499	-0.181	-0.178
c_8	0.844	0.813	0.799	0.740	-0.312	-0.297
c_9	-0.846	-0.815	-0.800	-0.744	0.615	0.611
A_{tot}	-0.070	-0.109	-0.127	-0.146	-0.010	-0.008
T_{rep}	NA	NA	NA	NA	0.484	0.483

References

Adams GE, Posener ML, Bisby RH, Cundall RB, Key JR. Free radical reactions with proteins and enzymes: the inactivation of pepsin. Int J Radiat Biol Relat Stud Phys Chem Med 1979;35:497–507. [PubMed: 383634]

Azzam EI, De Toledo SM, Spitz DR, Little JB. Oxidative metabolism modulates signal transduction and micronucleus formation in bystander cells from alpha-particle-irradiated normal human fibroblast cultures. Cancer Res 2002;62:5436–42. [PubMed: 12359750]

Barendsen GW. RBE-LET relationships for different types of lethal radiation damage in mammalian cells: comparison with DNA dsb and an interpretation of differences in radiosensitivity. Int J Radiat Biol 1994;66:433–6. [PubMed: 7983427]

Battista JR, Earl AM, Park MJ. Why is Deinococcus radiodurans so resistant to ionizing radiation? Trends Microbiol 1999;7:362–5. [PubMed: 10470044]

Bisby RH, Cundall RB, Movassaghi S, Adams GE, Posener ML, Wardman P. Selective free radical reactions with proteins and enzymes: a reversible equilibrium in the reaction of (SCN)2 radical with lysozyme. Int J Radiat Biol Relat Stud Phys Chem Med 1982;42:163–71. [PubMed: 6982249]

Blasius M, Sommer S, Hubscher U. Deinococcus radiodurans: what belongs to the survival kit? Crit Rev Biochem Mol Biol 2008;43:221–38. [PubMed: 18568848]

Brim H, Osborne JP, Kostandarithes HM, Fredrickson JK, Wackett LP, Daly MJ. Deinococcus radiodurans engineered for complete toluene degradation facilitates Cr(VI) reduction. Microbiology 2006;152:2469–77. [PubMed: 16849809]

Culard F, Gervais A, de Vuyst G, Spotheim-Maurizot M, Charlier M. Response of a DNA-binding protein to radiation-induced oxidative stress. J Mol Biol 2003;328:1185–95. [PubMed: 12729751]

Daly MJ. Modulating radiation resistance: Insights based on defenses against reactive oxygen species in the radioresistant bacterium Deinococcus radiodurans. Clin Lab Med 2006;26:491–504. [PubMed: 16815462]x

Daly MJ. A new perspective on radiation resistance based on Deinococcus radiodurans. Nat Rev Microbiol 2009;7:237–245. [PubMed: 19172147]

Daly MJ, Gaidamakova EK, Matrosova VY, Vasilenko A, Zhai M, Leapman RD, Lai B, Ravel B, Li SM, Kemner KM, Fredrickson JK. Protein oxidation implicated as the primary determinant of bacterial radioresistance. PLoS Biol 2007;5:e92. [PubMed: 17373858]

Daly MJ, Gaidamakova EK, Matrosova VY, Vasilenko A, Zhai M, Venkateswaran A, Hess M, Omelchenko MV, Kostandarithes HM, Makarova KS, Wackett LP, Fredrickson JK, Ghosal D. Accumulation of Mn(II) in Deinococcus radiodurans facilitates gamma-radiation resistance. Science 2004;306:1025–8. [PubMed: 15459345]

Dewey DL. The survival of Micrococcus radiodurans irradiated at high LET and the effect of acridine orange. Int J Radiat Biol Relat Stud Phys Chem Med 1969;16:583–92. [PubMed: 5308580]

Eon S, Culard F, Sy D, Charlier M, Spotheim-Maurizot M. Radiation disrupts protein-DNA complexes through damage to the protein. The lac repressor-operator system. Radiat Res 2001;156:110–7. [PubMed: 11418079]

Forman HJ, Torres M, Fukuto J. Redox signaling. Mol Cell Biochem 2002:234–235. 49–62.

Gerard E, Jolivet E, Prieur D, Forterre P. DNA protection mechanisms are not involved in the radioresistance of the hyperthermophilic archaea Pyrococcus abyssi and P. furiosus. Mol Genet Genomics 2001;266:72–8. [PubMed: 11589580]

Ghosal D, Omelchenko MV, Gaidamakova EK, Matrosova VY, Vasilenko A, Venkateswaran A, Zhai M, Kostandarithes HM, Brim H, Makarova KS, Wackett LP, Fredrickson JK, Daly MJ. How radiation kills cells: survival of Deinococcus radiodurans and Shewanella oneidensis under oxidative stress. FEMS Microbiol Rev 2005;29:361–75. [PubMed: 15808748]

Goodhead DT, Nikjoo H. Physical mechanism for inactivation of metallo-enzymes by characteristic X-rays: analysis of the data of Jawad and Watt. Int J Radiat Biol Relat Stud Phys Chem Med 1987;52:651–8. [PubMed: 2822588]

Haddad JJ. Redox and oxidant-mediated regulation of apoptosis signaling pathways: immuno-pharmaco-redox conception of oxidative siege versus cell death commitment. Int Immunopharmacol 2004;4:475–93. [PubMed: 15099526]

Hei TK. Cyclooxygenase-2 as a signaling molecule in radiation-induced bystander effect. Mol Carcinog 2006;45:455–60. [PubMed: 16637062]

Hess, M. Analysis of Deinococcus radiodurans mutants. Bethesda, MD: 2003.

Iliakis G, Wang H, Perrault AR, Boecker W, Rosidi B, Windhofer F, Wu W, Guan J, Terzoudi G, Pantelias G. Mechanisms of DNA double strand break repair and chromosome aberration formation. Cytogenet Genome Res 2004;104:14–20. [PubMed: 15162010]

Jolivet E, Lecointe F, Coste G, Satoh K, Narumi I, Bailone A, Sommer S. Limited concentration of RecA delays DNA double-strand break repair in Deinococcus radiodurans R1. Mol Microbiol 2006;59:338–49. [PubMed: 16359339]

Kasten-Pisula U, Tastan H, Dikomey E. Huge differences in cellular radiosensitivity due to only very small variations in double-strand break repair capacity. Int J Radiat Biol 2005;81:409–19. [PubMed: 16249159]

Kowalczyk A, Serafin E, Puchala M. Inactivation of chosen dehydrogenases by the products of water radiolysis and secondary albumin and haemoglobin radicals. Int J Radiat Biol 2008;84:15–22. [PubMed: 17852555]

Lange CC, Wackett LP, Minton KW, Daly MJ. Engineering a recombinant Deinococcus radiodurans for organopollutant degradation in radioactive mixed waste environments. Nat Biotechnol 1998;16:929–33. [PubMed: 9788348]

Liu Y, Zhou J, Omelchenko MV, Beliaev AS, Venkateswaran A, Stair J, Wu L, Thompson DK, Xu D, Rogozin IB, Gaidamakova EK, Zhai M, Makarova KS, Koonin EV, Daly MJ. Transcriptome

dynamics of Deinococcus radiodurans recovering from ionizing radiation. Proc Natl Acad Sci U S A 2003;100:4191–6. [PubMed: 12651953]

Makarova KS, Aravind L, Wolf YI, Tatusov RL, Minton KW, Koonin EV, Daly MJ. Genome of the extremely radiation-resistant bacterium Deinococcus radiodurans viewed from the perspective of comparative genomics. Microbiol Mol Biol Rev 2001;65:44–79. [PubMed: 11238985]

Makarova KS, Omelchenko MV, Gaidamakova EK, Matrosova VY, Vasilenko A, Zhai M, Lapidus A, Copeland A, Kim E, Land M, Mavrommatis K, Pitluck S, Richardson PM, Detter C, Brettin T, Saunders E, Lai B, Ravel B, Kemner KM, Wolf YI, Sorokin A, Gerasimova AV, Gelfand MS, Fredrickson JK, Koonin EV, Daly MJ. Deinococcus geothermalis: the pool of extreme radiation resistance genes shrinks. PLoS ONE 2007;2:e955. [PubMed: 17895995]

Makino N, Mise T, Sagara J. Kinetics of hydrogen peroxide elimination by astrocytes and C6 glioma cells analysis based on a mathematical model. Biochim Biophys Acta 2008;1780:927–36. [PubMed: 18402782]

Marino S, Hogue IB, Ray CJ, Kirschner DE. A methodology for performing global uncertainty and sensitivity analysis in systems biology. J Theor Biol 2008;254:178–96. [PubMed: 18572196]

Mennecier S, Servant P, Coste G, Bailone A, Sommer S. Mutagenesis via IS transposition in Deinococcus radiodurans. Mol Microbiol 2006;59:317–25. [PubMed: 16359337]

Mikkelsen R. Redox signaling mechanisms and radiation-induced bystander effects. Hum Exp Toxicol 2004;23:75–9. [PubMed: 15070064]

Montaner B, O'Donovan P, Reelfs O, Perrett CM, Zhang X, Xu YZ, Ren X, Macpherson P, Frith D, Karran P. Reactive oxygen-mediated damage to a human DNA replication and repair protein. EMBO Rep 2007;8:1074–9. [PubMed: 17932513]

Qiu X, Daly MJ, Vasilenko A, Omelchenko MV, Gaidamakova EK, Wu L, Zhou J, Sundin GW, Tiedje JM. Transcriptome analysis applied to survival of Shewanella oneidensis MR-1 exposed to ionizing radiation. J Bacteriol 2006;188:1199–204. [PubMed: 16428429]

Roots R, Holley W, Chatterjee A, Irizarry M, Kraft G. The formation of strand breaks in DNA after high-LET irradiation: a comparison of data from in vitro and cellular systems. Int J Radiat Biol 1990;58:55–69. [PubMed: 1973440]

Rugo RE, Secretan MB, Schiestl RH. X radiation causes a persistent induction of reactive oxygen species and a delayed reinduction of TP53 in normal human diploid fibroblasts. Radiat Res 2002;158:210–9. [PubMed: 12105992]

Saha A, Mandal PC, Bhattacharyya SN. Radiation-induced inactivation of dihydroorotate dehydrogenase in dilute aqueous solution. Radiat Res 1992;132:7–12. [PubMed: 1410277]

Saleh EM, El-Awady RA. Misrejoined, residual double strand DNA breaks and radiosensitivity in human tumor cell lines. J Egypt Natl Canc Inst 2005;17:93–102. [PubMed: 16508680]

Sangsuwan T, Haghdoost S. The nucleotide pool, a target for low-dose gamma-ray-induced oxidative stress. Radiat Res 2008;170:776–83. [PubMed: 19138035]

Sasaki K, Bannai S, Makino N. Kinetics of hydrogen peroxide elimination by human umbilical vein endothelial cells in culture. Biochim Biophys Acta 1998;1380:275–88. [PubMed: 9565698]

Schimmel M, Bauer G. Proapoptotic and redox state-related signaling of reactive oxygen species generated by transformed fibroblasts. Oncogene 2002;21:5886–96. [PubMed: 12185588]

Shukla M, Chaturvedi R, Tamhane D, Vyas P, Archana G, Apte S, Bandekar J, Desai A. Multiple-stress tolerance of ionizing radiation-resistant bacterial isolates obtained from various habitats: correlation between stresses. Curr Microbiol 2007;54:142–8. [PubMed: 17180747]

Spitz DR, Azzam EI, Li JJ, Gius D. Metabolic oxidation/reduction reactions and cellular responses to ionizing radiation: a unifying concept in stress response biology. Cancer Metastasis Rev 2004;23:311–22. [PubMed: 15197331]

Tominaga H, Kodama S, Matsuda N, Suzuki K, Watanabe M. Involvement of reactive oxygen species (ROS) in the induction of genetic instability by radiation. J Radiat Res (Tokyo) 2004;45:181–8. [PubMed: 15304958]

Ward JF. The yield of DNA double-strand breaks produced intracellularly by ionizing radiation: a review. Int J Radiat Biol 1990;57:1141–50. [PubMed: 1971840]

White O, Eisen JA, Heidelberg JF, Hickey EK, Peterson JD, Dodson RJ, Haft DH, Gwinn ML, Nelson WC, Richardson DL, Moffat KS, Qin H, Jiang L, Pamphile W, Crosby M, Shen M, Vamathevan JJ,

Lam P, McDonald L, Utterback T, Zalewski C, Makarova KS, Aravind L, Daly MJ, Minton KW, Fleischmann RD, Ketchum KA, Nelson KE, Salzberg S, Smith HO, Venter JC, Fraser CM. Genome sequence of the radioresistant bacterium Deinococcus radiodurans R1. Science 1999;286:1571–7. [PubMed: 10567266]

Zahradka K, Slade D, Bailone A, Sommer S, Averbeck D, Petranovic M, Lindner AB, Radman M. Reassembly of shattered chromosomes in Deinococcus radiodurans. Nature 2006;443:569–73. [PubMed: 17006450]

Zhang C, Wei J, Zheng Z, Ying N, Sheng D, Hua Y. Proteomic analysis of Deinococcus radiodurans recovering from gamma-irradiation. Proteomics 2005;5:138–43. [PubMed: 15593145]

Zimmermann H, Schafer M, Schmitz C, Bucker H. Effects of heavy ions on inactivation and DNA double strand breaks in Deinococcus radiodurans R1. Adv Space Res 1994;14:213–6. [PubMed: 11539954]
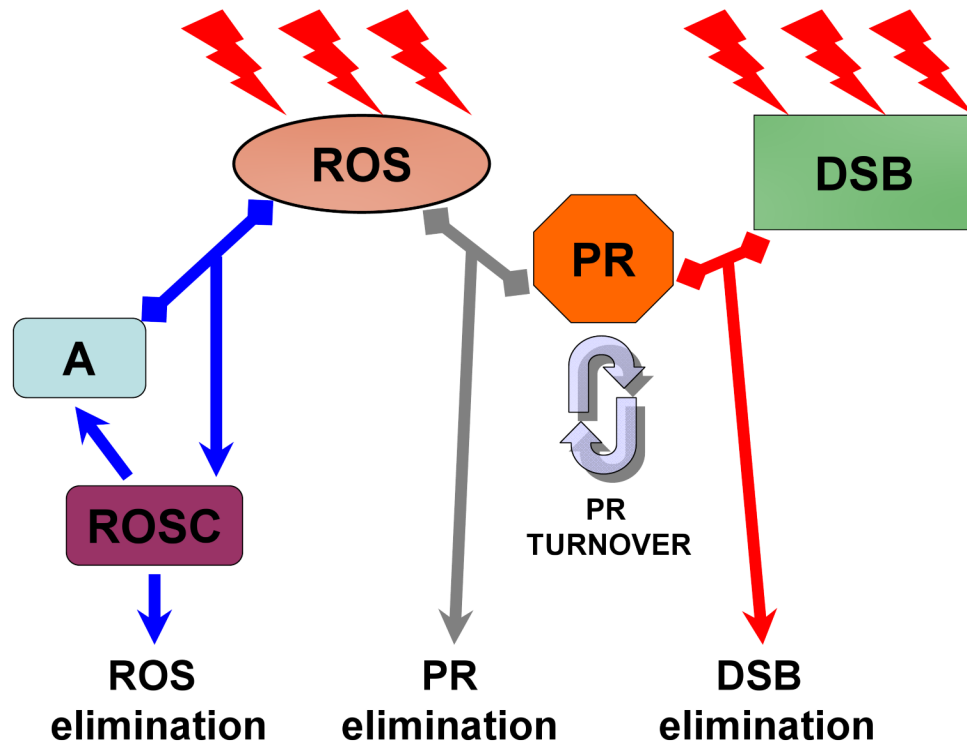
Fig. 1.
Schematic representation of model assumptions: Radiation (lightning symbols) produces reactive oxygen species (ROS) and DNA double strand breaks (DSB). ROS can react with antioxidants (A) to form a complex (ROSC), which then decays, resulting in elimination of ROS and regeneration of the antioxidants. DSBs are eliminated by repair involving specific proteins (PR), which are produced and degraded at a certain turnover rate. Importantly, ROS can damage these proteins, resulting in elimination of their repair capacity. Consequently, those ROS that are not removed by antioxidants damage DNA repair machinery and hinder correct repair of DSBs. Details are discussed throughout the main text.
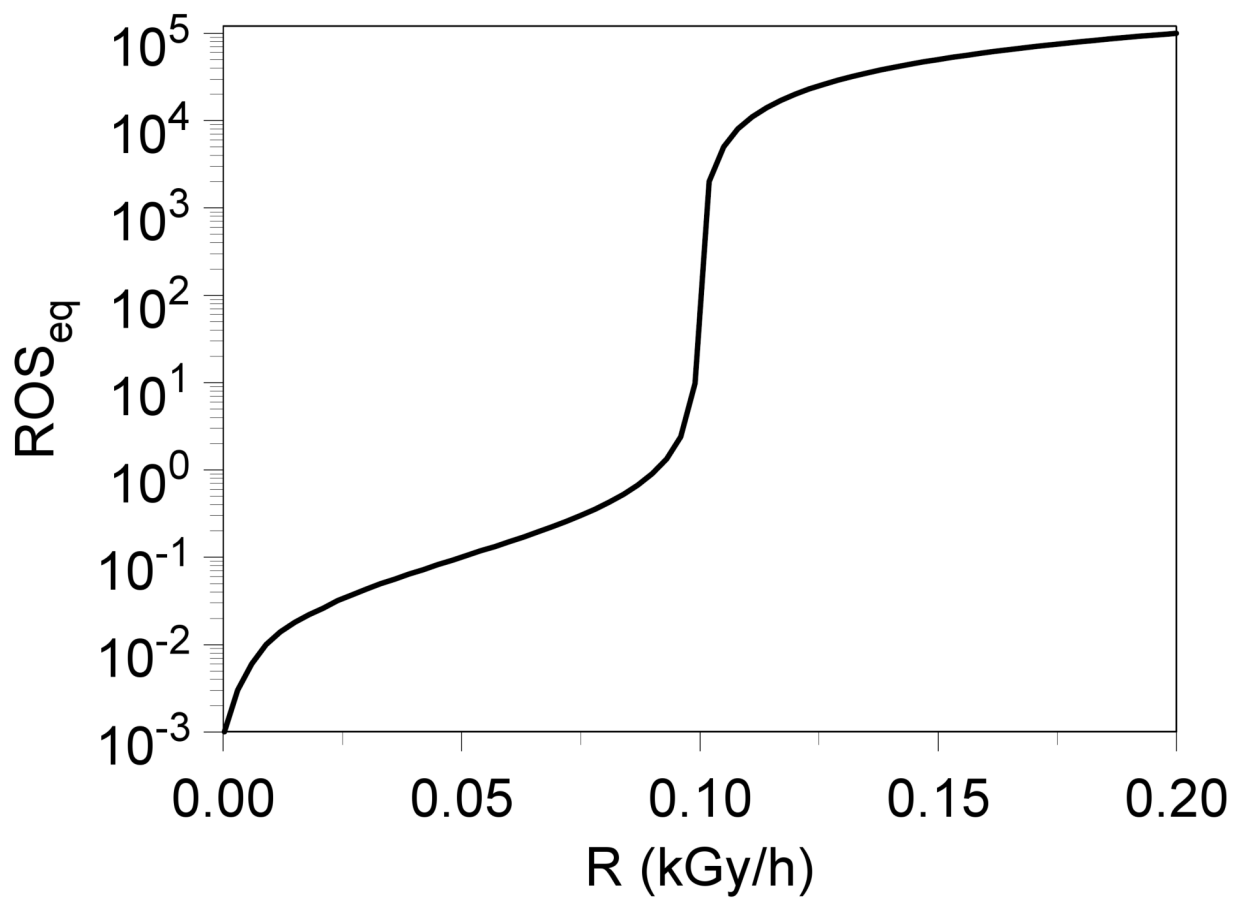
Fig. 2.
The predicted equilibrium concentration of reactive radicals (ROS_{eq}, in arbitrary units) during irradiation at a constant dose rate (R).
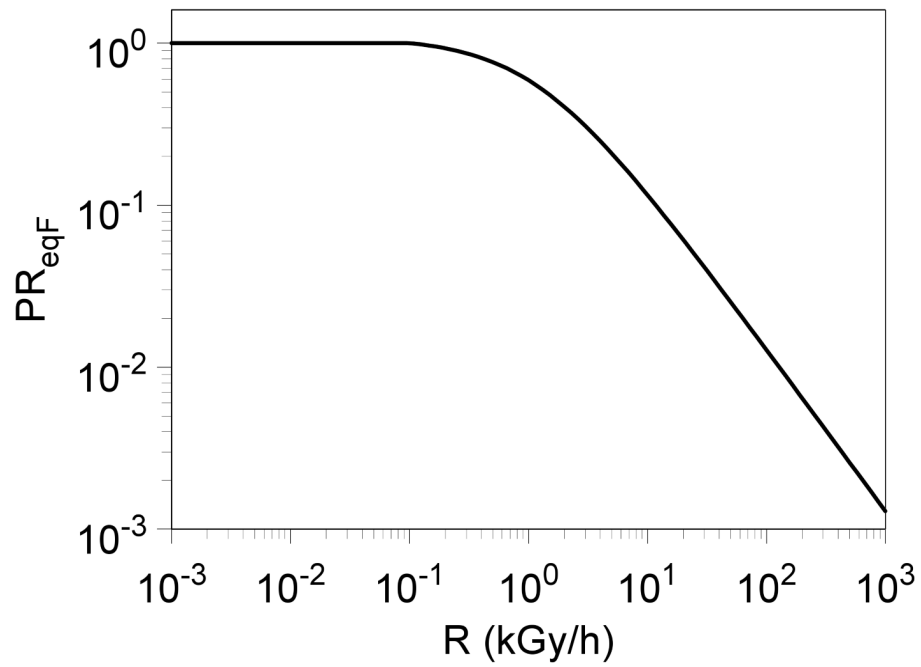
Fig. 3.
The predicted equilibrium concentration of active protein, normalized relative to the equilibrium concentration under background conditions (i.e. $PR_{eqF} = PR_{eq}/[c_5/c_6]$) during irradiation at a constant dose rate (R).
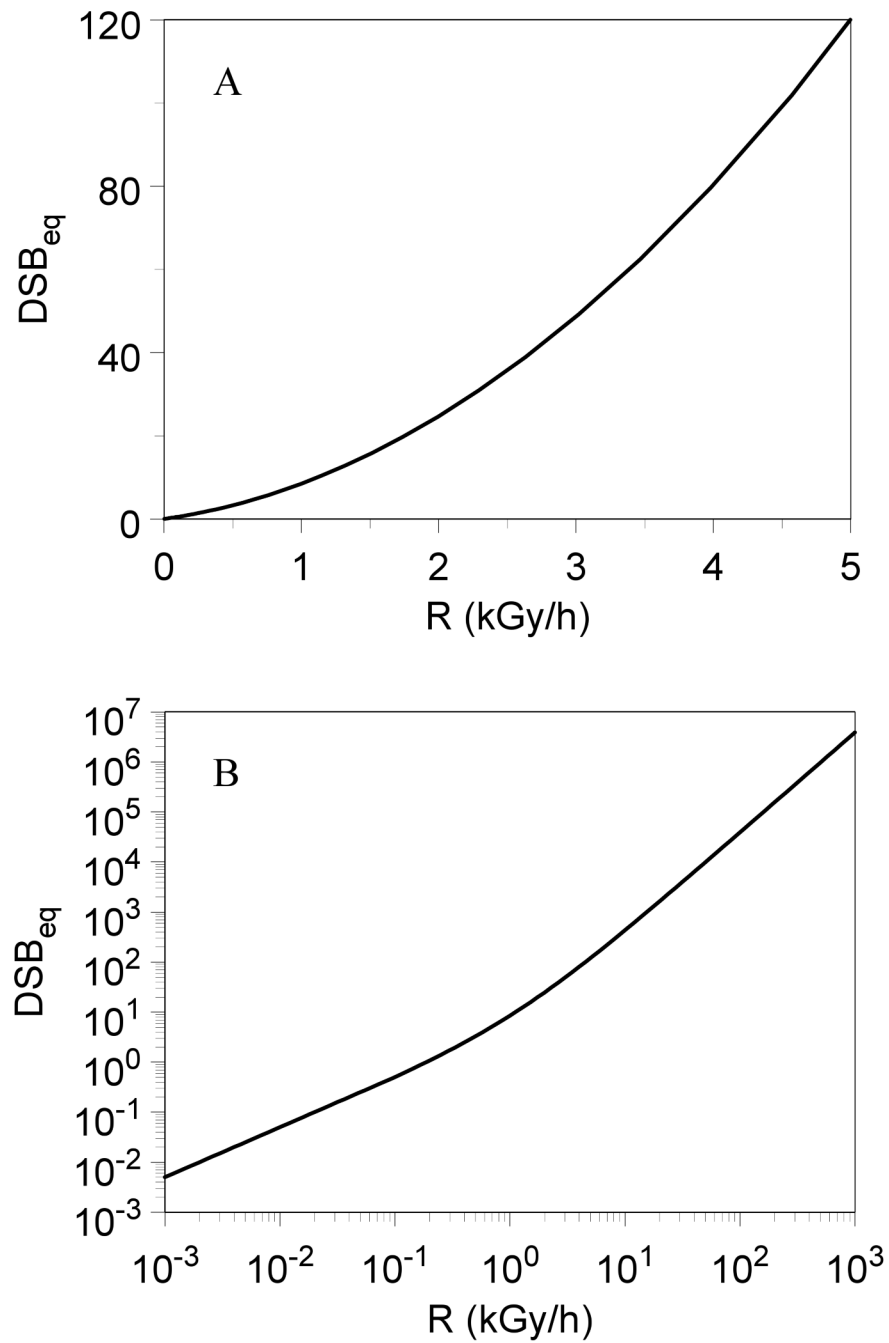
Fig. 4.
The predicted equilibrium number of DNA DSBs per cell (DSB_{eq}) during irradiation at a constant dose rate (R). Panel A shows the results up to 5 kGy/h, and panel B shows the results up to 1000 kGy/h (i.e. acute exposure).
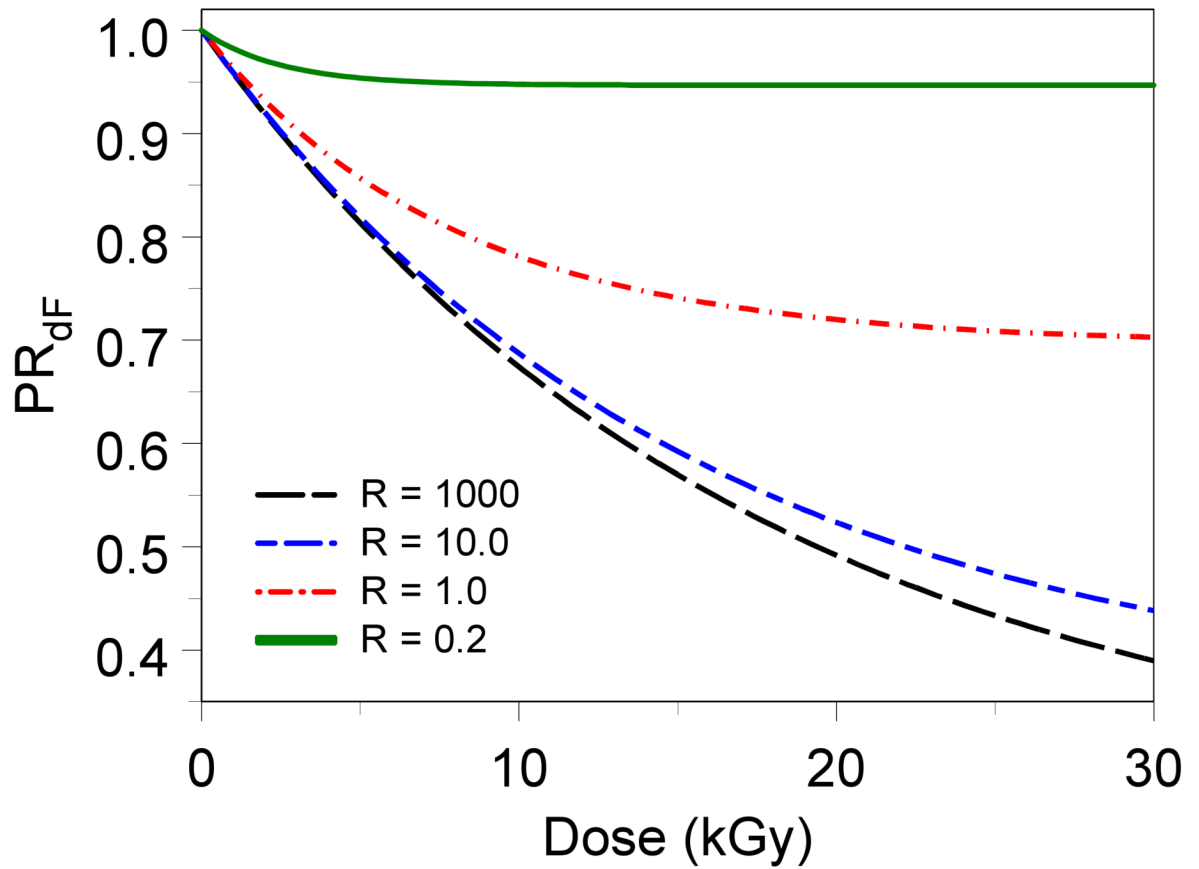
Fig. 5.
The predicted fraction of active protein, normalized relative to the background equilibrium value (i.e. $PR_{dF} = PR_d/[c_5/c_6]$) just after radiation exposure at various doses (in kGy) and dose rates (R, in kGy/h).
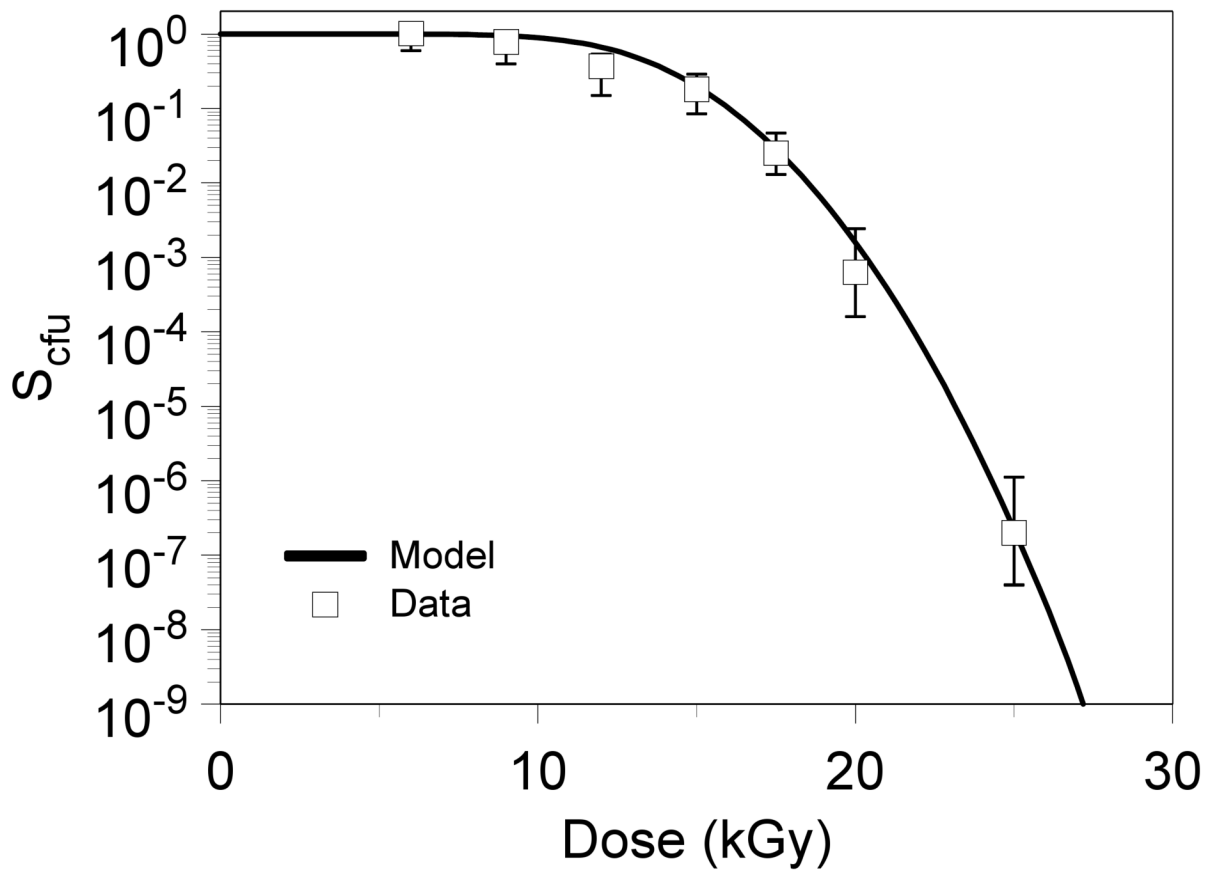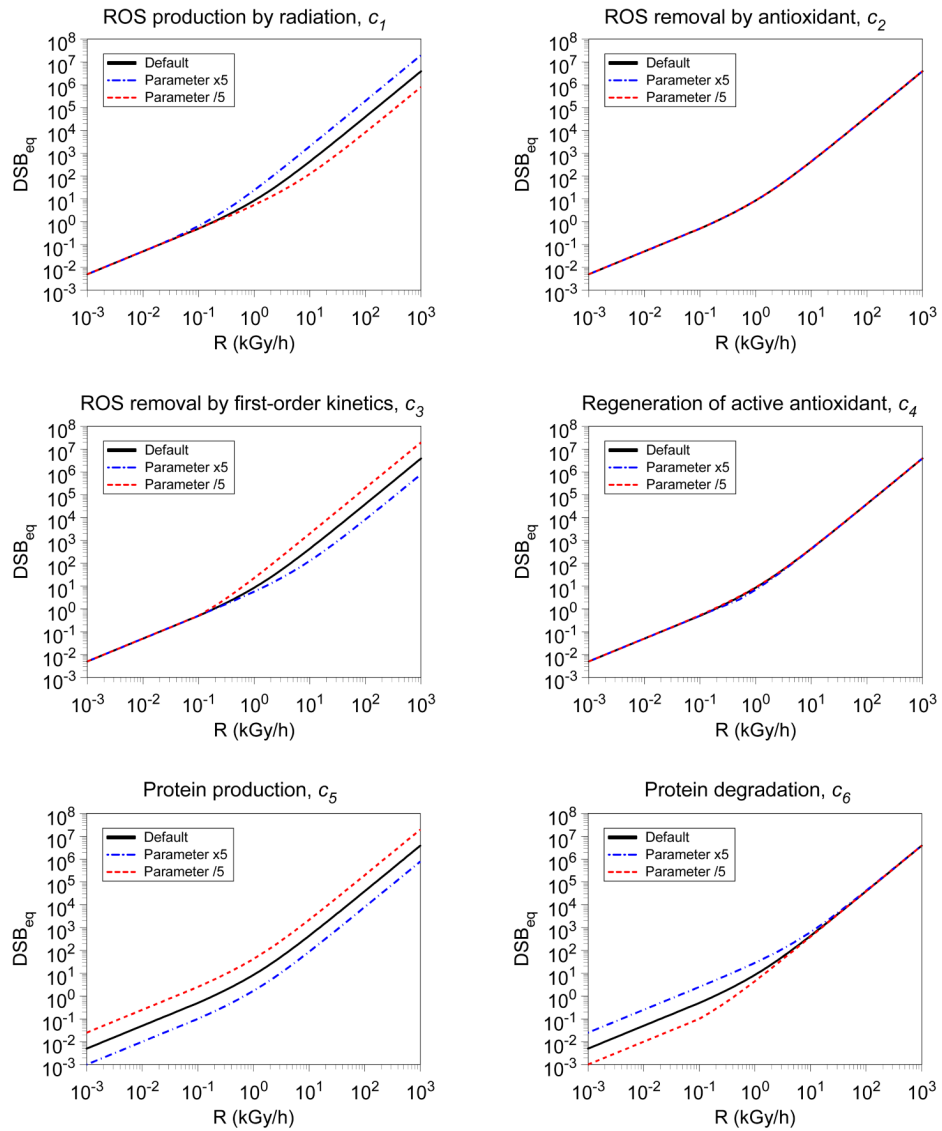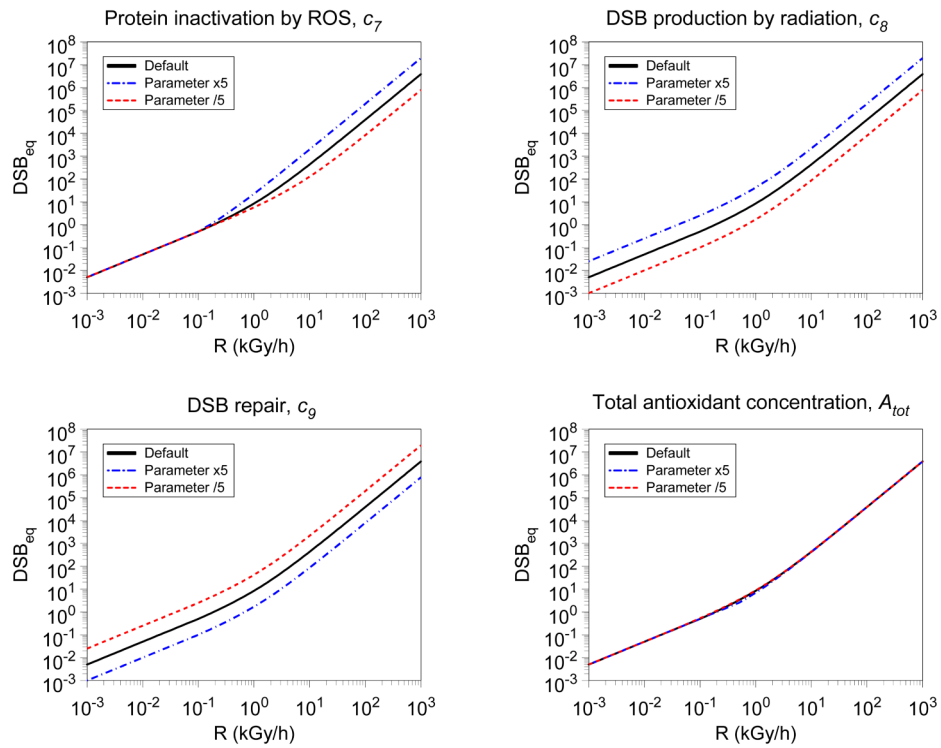
Fig. 6.
The predicted colony-forming unit survival (S_{cfu}) for *D. radiodurans* exposed to acute γ-radiation (on ice) in complete growth medium (curve), compared with observed data points from (Daly et al., 2004).
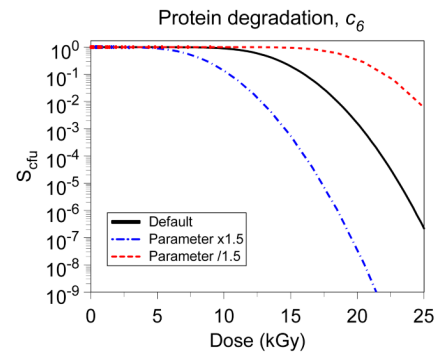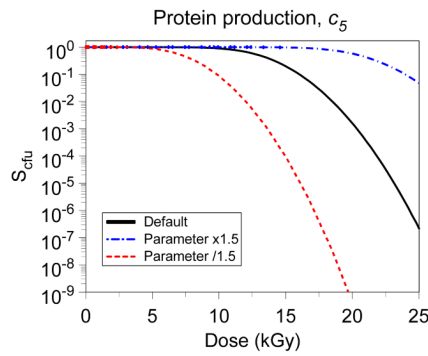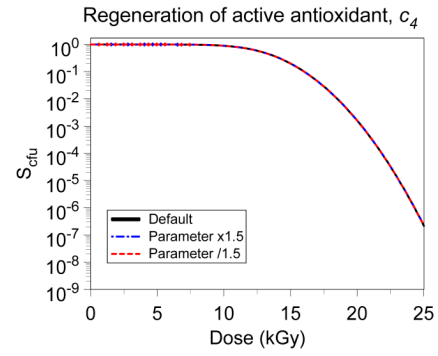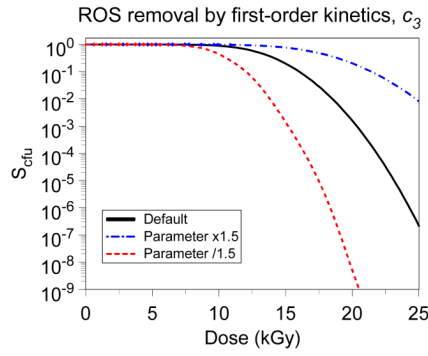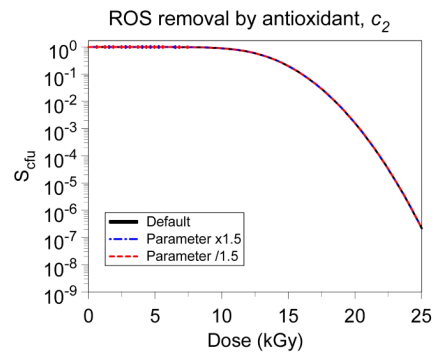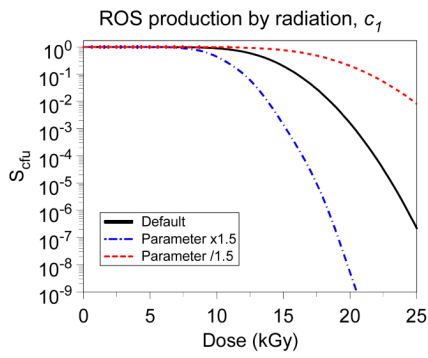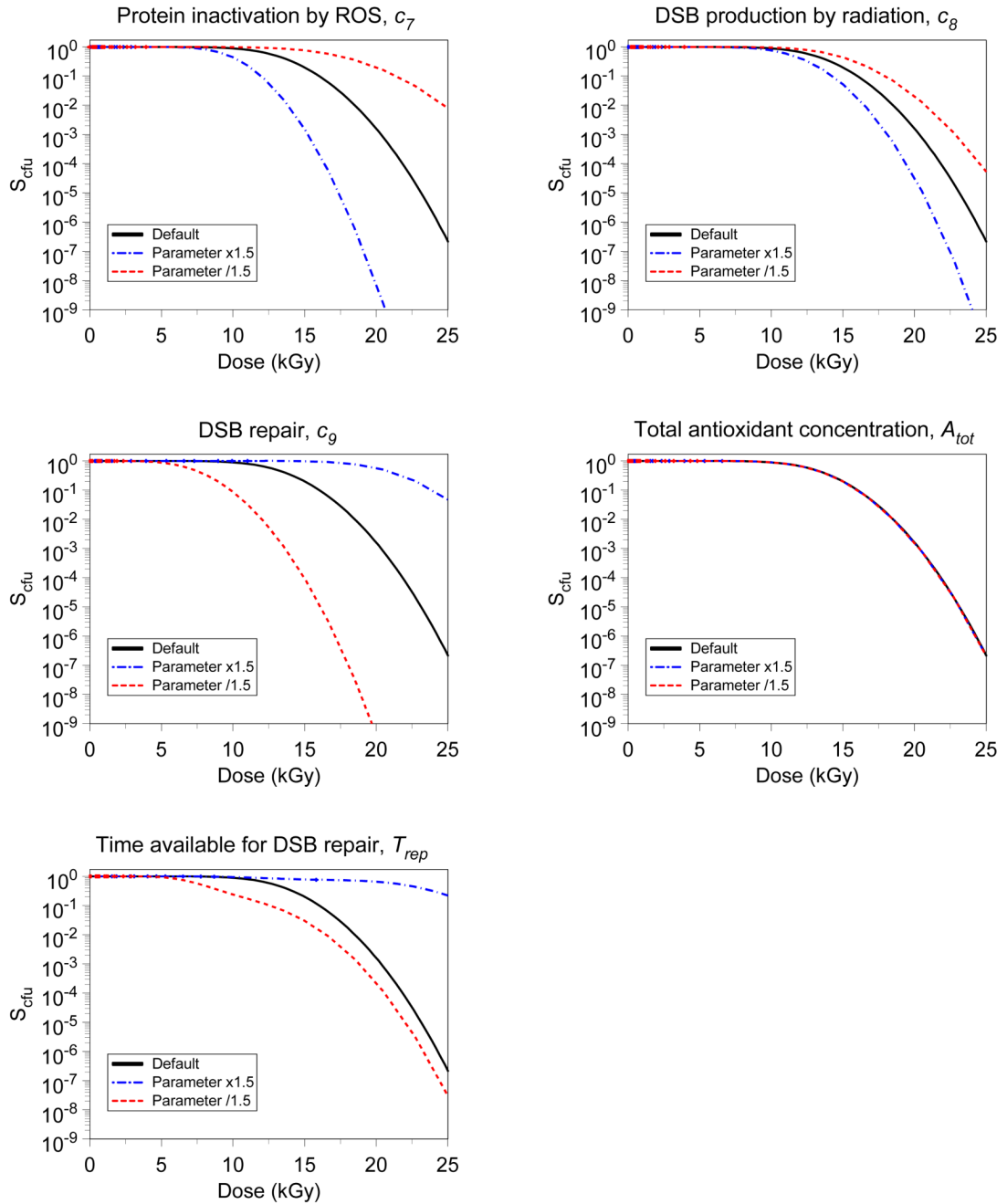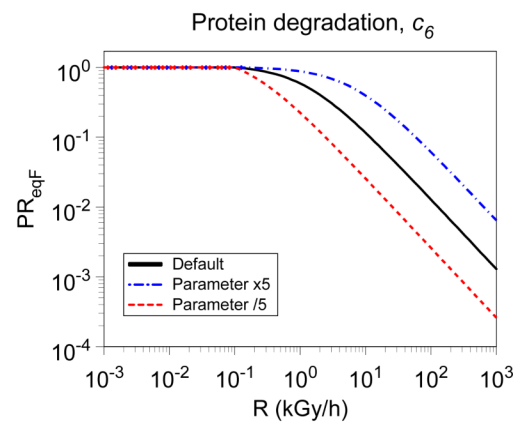
Fig. 7.
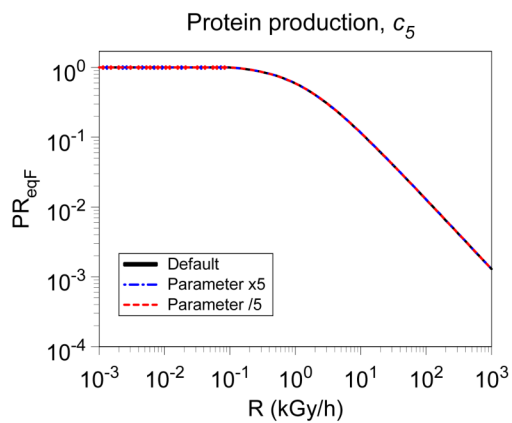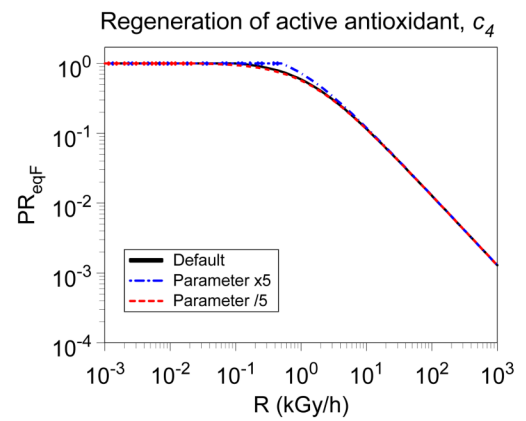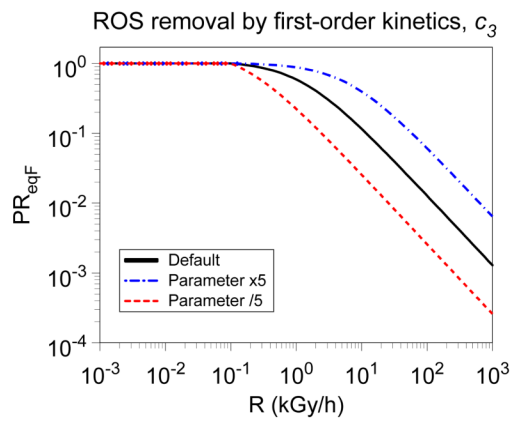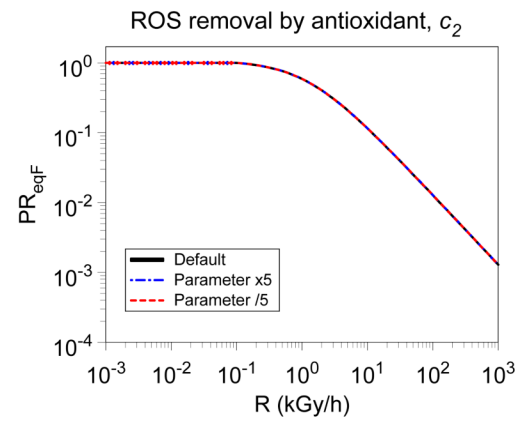Parameter sensitivities – effect on colony-forming unit survival after acute irradiation. Black curve = default parameter values from Table 1. Blue curve = increasing the selected parameter by a factor of 1.5, while keeping all other parameters constant. Red curve = decreasing the selected parameter by a factor of 1.5, while keeping all other parameters constant. In some panels in this and the following two figures, only one curve is visible – this occurs when the given parameter has only a marginal effect on model predictions, so all three curves overlap.

ROS production by radiation, c_1

ROS removal by antioxidant, c_2

ROS removal by first-order kinetics, c_3

Regeneration of active antioxidant, c_4

Protein production, c_5

Protein degradation, c_6

Fig. 8.
Parameter sensitivities – effect on equilibrium number of DSBs during chronic irradiation. Black curve = default parameter values from Table 1. Blue curve = increasing the selected parameter by a factor of 5, while keeping all other parameters constant. Red curve = decreasing the selected parameter by a factor of 5, while keeping all other parameters constant.

ROS production by radiation, c_1

ROS removal by antioxidant, c_2

ROS removal by first-order kinetics, c_3

Regeneration of active antioxidant, c_4

Protein production, c_5

Protein degradation, c_6
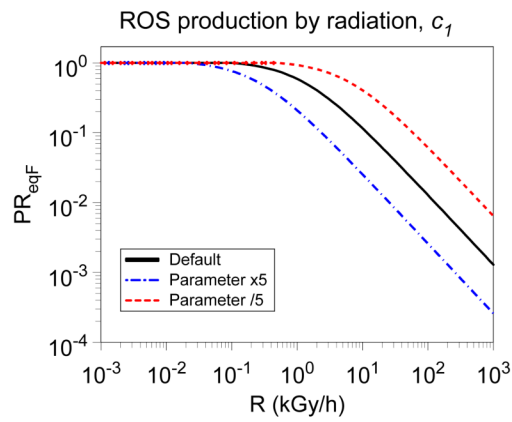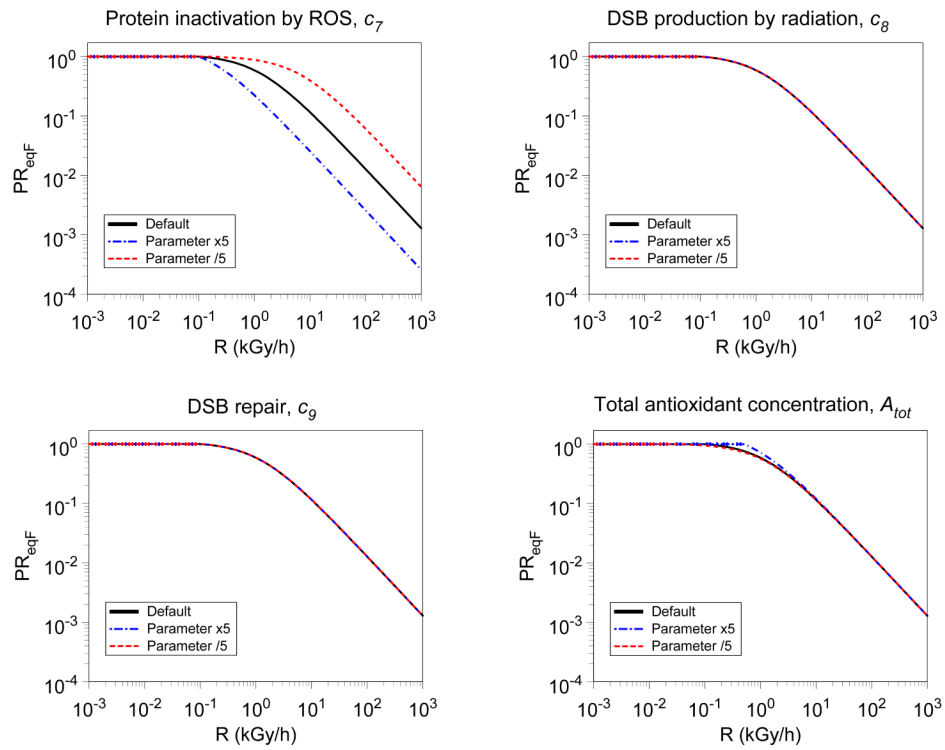
Fig. 9.
Parameter sensitivities – effect on equilibrium active protein concentration (normalized relative to the background equilibrium c_5/c_6) during chronic irradiation. Black curve = default parameter values from Table 1. Blue curve = increasing the selected parameter by a factor of 5, while keeping all other parameters constant. Red curve = decreasing the selected parameter by a factor of 5, while keeping all other parameters constant.

Table 1

Default model parameter values and interpretations. Parameters c_8 and c_9 were estimated from the literature (Daly et al., 2007; Daly et al., 2004; Lange et al., 1998; Zahradka et al., 2006), and for the remaining ones arbitrary values were used. These values were manually adjusted to generate model predictions consistent with the observed survival of *D. radiodurans* after acute or chronic γ-irradiation, from the same references.

Parameter	Interpretation	Default value
c_1	ROS production by radiation	1.0×10^6 concentration$\times$kGy^{-1}
c_2	ROS removal by antioxidant	1.0×10^6 concentration^{-1}$\times$h^{-1}
c_3	ROS removal by first-order kinetics	1.0 h^{-1}
c_4	Regeneration of active antioxidant	1.0×10^5 h^{-1}
c_5	Protein production	0.1 concentration$\times$h^{-1}
c_6	Protein degradation	0.075 h^{-1}
c_7	Protein inactivation by ROS	5.8×10^{-8} concentration^{-1}$\times$h^{-1}
c_8	DSB production by radiation	10.0 breaks $\times$cell^{-1}$\times$kGy^{-1}
c_9	DSB repair	1.5 concentration^{-1}$\times$h^{-1}
A_{tot}	Total antioxidant concentration	1.0 concentration
T_{rep}	Time available for DSB repair	4.0 h

Table 2

Effects of varying parameter values on the shape of the survival curve for colony-forming units (S_{cfu}). $Dose_{90}$ refers to the acute radiation dose (in kGy) required to reduce S_{cfu} to 90%; it is an estimate of the length of the "shoulder" of the survival curve. $Slope_{20}$ refers to the Log_{10} reduction in S_{cfu} per kGy at a dose of 20 kGy; it is an estimate of the "terminal slope" of the survival curve. The column labeled "default" contains the predicted values of $Dose_{90}$ and $Slope_{20}$ using default parameter values from Table 1. The other columns contain ratios for $Dose_{90}$ and $Slope_{20}$, relative to default values, calculated by first increasing, and then decreasing the given parameter by a factor of 1.5. For example, if parameter c_1 is increased 1.5-fold, $Dose_{90}$ decreases by a factor of 0.75; if c_1 is decreased 1.5-fold, $Dose_{90}$ increases by a factor of 1.32.

	Default	c_1	c_2	c_3	c_4	c_5	c_6	c_7	c_8	c_9	A_{tot}	T_{rep}
$Dose_{90}$	9.82	0.75	1.00	1.32	1.00	1.72	0.49	0.75	0.88	1.72	1.00	1.13
		1.32	1.00	0.75	1.00	0.47	1.70	1.32	1.13	0.47	1.00	0.54
$Slope_{20}$	0.62	2.27	1.00	0.33	1.00	0.21	1.73	2.27	1.50	0.21	1.00	0.07
		0.33	1.00	2.27	1.00	2.42	0.36	0.33	0.66	2.42	1.00	1.00